

Brief Communication

De novo creation of narrowed plant architecture via CRISPR/Cas9-mediated mutagenesis of *SiLGs* in foxtail millet

Renliang Zhang¹, Ruifeng Guo², Hui Zhi¹, Sha Tang¹, Liwei Wang¹, Yuemei Ren², Guangbing Ren², Shou Zhang², Jing Feng², Xianmin Diao^{1,3,*}  and Guanqing Jia^{1,3,*} 

¹State Key Laboratory of Crop Gene Resources and Breeding/Key laboratory Grain Crop Genetic Resources Evaluation and Utilization Ministry of Agriculture and Rural Affairs/Institute of Crop Sciences, CAAS, Beijing, China

²Crops Research Institute in Severe Cold Region, Shanxi Agricultural University, Datong, Shanxi, China

³Zhongyuan Research Center, Chinese Academy of Agricultural Sciences, Xinxiang, China

Received 2 July 2024;

revised 19 February 2025;

accepted 25 February 2025.

*Correspondence (Tel +861062126889; Fax +861062126889;

email jiaguanqing@caas.cn (G.J.);

Tel +861062126889; Fax +861062126889; email diaoxianmin@caas.cn (X.D.))

Keywords: Foxtail millet, plant architecture, *SiLG1*, *SiLG2*.

Foxtail millet [*Setaria italica* (L.) Beauv] is an ancient cereal crop that has been cultivated for grain food and forage consumption globally for over 11 500 years. Despite its long history, foxtail millet continues to be extensively cultivated in developing and underdeveloped countries with low productivity conditions. This is primarily due to its exceptional ability to tolerate drought and barren environments, making it well-suited for grain production in challenging grown conditions. In the last century, significant progress has been made in enhancing the plant architecture of major cereal crops, such as maize (*Zea mays*) and rice (*Oryza sativa*), resulting in substantial increases in grain yield potential (Tian *et al.*, 2024). However, there has been relatively less emphasis on optimizing the plant architecture of foxtail millet, leading to limited improvements in yield for this ancient crop species to date. While the overexpression of *Drooping Leaf 1* has been shown to promote more upright leaves in foxtail millet (Zhao *et al.*, 2020), compact architecture with reduced leaf angle remains a challenge due to the scarcity of identified germplasm suitable for this purpose.

Leaf angle, defined as the angle between the culm and leaf midrib, is a crucial aspect of plant architecture that is controlled by a limited number of functional genes. Among these genes, *Liguleless1* (*LG1*) and *Liguleless2* (*LG2*) are key regulators that play essential roles in lamina joint formation, influencing leaf angle in maize (Walsh *et al.*, 1998). *LG1* has been identified as a transcription factor belonging to the Squamosa Promoter-Binding Proteins (SBP) family, while *LG2* has been characterized as a basic leucine zipper transcription (bZIP) factor. Genetic analysis of variations indicates that *LG1* and *LG2* have the potential to significantly enhance the field productivity of maize varieties, and

it has been demonstrated that the functions of *LG1* and *LG2* are conserved across various Gramineae crops, including maize (Harper and Freeling, 1996), rice (Wang *et al.*, 2021), wheat (Yu, 2019), sorghum (Brant *et al.*, 2021) and sugarcane (Brant *et al.*, 2024). However, the roles of *LG1* and *LG2* in foxtail millet remain unclear, and as of now, no ligule development-defective mutants have been identified in this coarse cereal crop.

In this study, *SiLG1* and *SiLG2* were identified in foxtail millet through phylogenetic analysis (Figure S1). Both of *SiLG1* and *SiLG2* were mainly expressed in leaves, pulvinus, nodes and seeds of foxtail millet (Figure S2). A comprehensive screening analysis was conducted on sequencing data of 1844 worldwide *Setaria italica* germplasm, which included commercial varieties, landraces, and wild relatives (He *et al.*, 2024, www.setariadb.com/millet), and the allelic variations and the prevalence of *SiLG1* and *SiLG2* in this crop species (Figure 1a, Table S1) were then assessed by geneHapR software (Zhang *et al.*, 2023).

A total of five nucleotide polymorphisms, comprising one insertion–deletion (indel) and four single-nucleotide substitutions (SNPs) within intronic and exonic regions, were identified in *SiLG1* (Figure 1b). The exonic mutations included one synonymous variant and a missense mutation (p.Pro110Gln), both of which did not affect the SBP domain of the *SiLG1* protein (Figure 1b, Figure S3a). All accessions were classified into five groups of haplotypes (H001 to H005) based on their allelic frequencies (Table S2). Haplotype H001 was primarily found in cultivated varieties, while H002 was prevalent in wild accessions. Haplotypes H003, H004, and H005 were exclusively identified in wild accessions. Phenotypic comparisons between H001 and H002 of *SiLG1* in foxtail millet cultivars, encompassing traits such as leaf angle, leaf length, leaf width, and plant height surveyed from diverse locations and years (www.setariadb.com/millet), revealed no significant differences ($P < 0.001$ by Student's *t*-test). Moreover, a total of 31 nucleotide polymorphisms were observed in the genomic region of *SiLG2* (Figure 1c). Among these, two were located in exonic regions, including a missense mutation (p.Ala197Pro) in the ninth exon preceding the bZIP domain of the *SiLG2* protein (Figure S3b), along with a synonymous variant (Table S3). Nine haplotypes were identified in *SiLG2*, with only H001 identified in cultivars (Table S3).

Please cite this article as: Zhang, R., Guo, R., Zhi, H., Tang, S., Wang, L., Ren, Y., Ren, G., Zhang, S., Feng, J., Diao, X. and Jia, G. (2025) De novo creation of narrowed plant architecture via CRISPR/Cas9-mediated mutagenesis of *SiLGs* in foxtail millet. *Plant Biotechnol. J.*, <https://doi.org/10.1111/pbi.70037>.

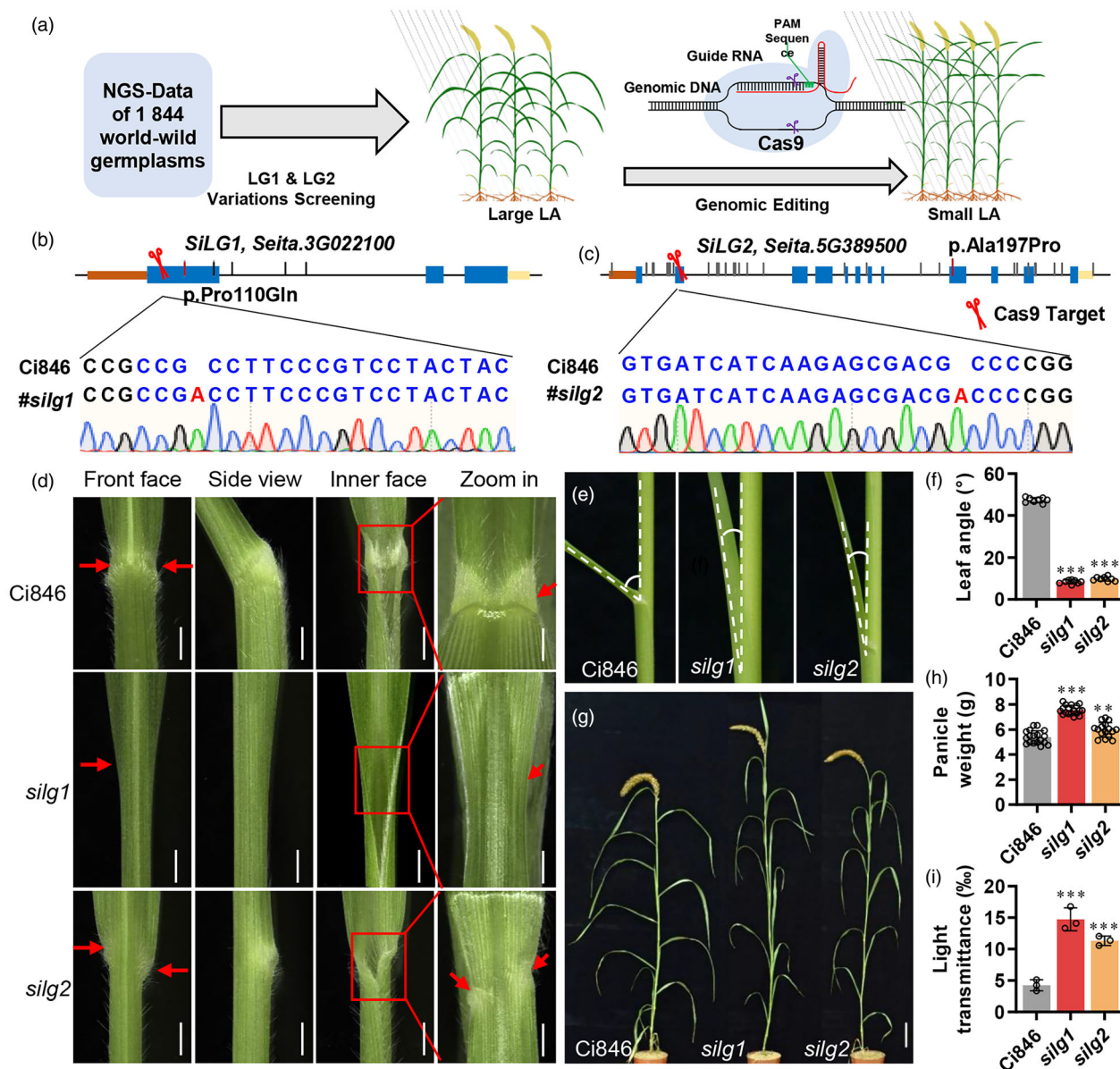


Figure 1 Creation of narrowed plant architecture in foxtail millet using the clustered regularly interspaced palindromic repeats (CRISPR)/CRISPR-associated protein 9 (Cas9) technique. (a) Technical diagram of experimental design. (b, c) Positions of natural variants and genomic editing of *SILG1* (b) and *SILG2* (c). Black vertical lines indicate variants not influence the amino acids while red vertical lines indicate missense mutations. The “p.Pro110Gln” and “p.Ala197Pro” represent 110th Proline substituted to Glutamine and 197th Alanine substituted to Proline, respectively. Red arrow indicates position of gene editing targets. Nucleotides sequences in black colour represent PAM sequences and the blue sequence indicate targets while red colour means insertion. (d) Phenotype of *silg1* and *silg2* panicles. Red arrows indicated the position of auricle regions. Bar = 2 mm. (e) Leaf angle variations of *silg1* and *silg2*. (f) Statistics of leaf angle of Ci846, *silg1* and *silg2*. (g) Individuals of Ci846, *silg1* and *silg2*. Bar = 10 cm. (h, i) Statistics of panicle weight (h) and light transmittance (i) of Ci846, *silg1* and *silg2*. ** and *** represents $P < 0.01$ and $P < 0.001$ by Student's *t*-test, respectively.

Considering that ligule developmental defects in foxtail millet have not been previously characterized and leaf ligule formation remains unaffected by the missense variants identified in *SILG1* and *SILG2*, it presents an effective strategy to generate germplasm with reduced leaf angle and compact plant architecture by introducing novel alleles of *SILG1* and *SILG2* into foxtail millet utilizing genome editing techniques for breeding initiatives targeting this coarse cereal crop. To accomplish this goal, sgRNAs targeting *SILG1* and *SILG2* were designed and incorporated into the pYLCRISPR/Cas9-Pubi-H vector. Subsequently, these constructs were introduced into Ci846, a foxtail millet cultivar, via

Agrobacterium-mediated transformation (Figure 1b, c) to disrupt *SILG1* and *SILG2*. A total of 9 transgenic lines containing the CRISPR/Cas9 vector targeting *SILG1* were obtained and confirmed through PCR analysis. Sequencing analysis revealed that all the 8 edited lines of *SILG1* possessed an insertion of a single base pair “A” (Figure 1b), leading to premature termination before the SBP domain (Figure S3a). The homozygous genome-edited *SILG1* lines (referred to as *silg1* hereafter) exhibited a complete absence of ligule, auricle region, and lamina joint, with a reduced leaf angle of approximately 8 $^{\circ}$ (Figure 1d–f). Moreover, two edited lines showed an “A” insertion (referred to as *silg2* hereafter),

causing the deletion of the bZIP domain in *SilG2* (Figure S3b), resulting in missing ligule but retaining the auricle region with incorrect positioning (Figure 1d, e). Additionally, the leaf angle of *silg2* was decreased to around 10° (Figure 1f).

To assess the agronomic traits of *silg1* and *silg2*, nine traits, including plant height, leaf length, leaf width, panicle diameter, panicle length, yield per hectare, seed length, seed width and 1000-seeds weight, were measured in Cas9-free lines derived from genome-edited individuals of *silg1* and *silg2* (Table S4). Our findings revealed that the *silg1* mutants were taller than wild type (WT), while the leaf length and width remained comparable (Figure 1g, Figure S4a–c). Intriguingly, in the *silg1* mutant, although the panicle diameter was smaller, both grain weight and panicle weight exceeded those of Ci846 due to increased panicle compactness (Figure 1h, Figure S4d, e). Furthermore, the 1000-seeds weight of the *silg1* mutant decreased because of reduced seed width and seed length, whereas in the *silg2* mutant, it increased due to enhanced seed length (Figure S5). Moreover, under field conditions, the light transmittance in *silg1* and *silg2* mutants exceeded those of WT (Figure 1i). Notably, in the field experiments conducted in Datong in 2023 and 2024, both of *silg1* and *silg2* showed higher grain yield than WT of Ci846 at the density of 240 000 individuals per hectare (Figure S4f, g).

As illustrated in Figure S6, the indole-3-acetic acid (IAA) content exhibited a notable decrease in the *silg1* and *silg2* mutants compared to the WT. Conversely, the tryptophan (TRP) content in WT surpassed that of the mutants. Additionally, the oxindole-3-acetic acid (OxIAA) content was higher in WT than in the mutants. The levels of the conjugated forms IAA-Gly and IAA-Glc were elevated in *silg1* and *silg2*, particularly in *silg2*. Furthermore, transcriptomic analysis unveiled an inhibition of auxin synthesis and signalling in *silg1* and *silg2* (Figure S7), and three PIN genes containing *LG1* binding motifs in their promoters showed altered expression in *silg1* compared with WT (Figure S8).

In conclusion, our study has successfully utilized genome editing techniques to introduce novel alleles of *SilG1* and *SilG2* into foxtail millet with the aim of enhancing its plant architecture beyond what is naturally present in germplasm collections. The functional loss of *SilG1* resulted in the absence of the ligule, auricle region, and lamina joint, while mutations in *SilG2* led to developmental defects in the lamina joint, retaining the auricle region albeit often in mis-positioned configurations. Field-based phenotypic assessments of *silg1* and *silg2* have confirmed the efficacy of the newly created alleles as potentially valuable genetic assets for elevating the yield potential of foxtail millet by increasing plant density through a more compact architectural framework.

Acknowledgements

This study was supported by the National Key Research and Development Program of China (2023YFD1200705/

2023YFD1200700), National Natural Science Foundation of China (32341032), The IAEA Coordinated Research Project (D24016), China Agricultural Research System (CARS06-14.5-A04), Key Laboratory of Crop Gene Resource and Germplasm Enhancement (MOA), Technology Innovation Program of CAAS.

Data availability statement

The sequencing data have been deposited on ngdc.cncb.ac.cn (Bio-project Accession ID: PRJCA034863).

References

- Brant, E., Baloglu, M., Parikh, A. and Altpeter, F. (2021) CRISPR/Cas9 mediated targeted mutagenesis of *LIGULELESS-1* in sorghum provides a rapidly scorable phenotype by altering leaf inclination angle. *Biotechnol. J.* **16**, e2100237.
- Brant, E., Eid, A., Kannan, B., Baloglu, M. and Altpeter, F. (2024) The extent of multiallelic, co-editing of *LIGULELESS1* in highly polyploid sugarcane tunes leaf inclination angle and enables selection of the ideotype for biomass yield. *Plant Biotechnol. J.* **22**, 2660–2671.
- Harper, L. and Freeling, M. (1996) Interactions of *liguleless1* and *liguleless2* function during ligule induction in maize. *Genetics* **144**, 1871–1882.
- He, Q., Wang, C., He, Q., Zhang, J., Liang, H., Lu, Z. *et al.* (2024) A complete reference genome assembly for foxtail millet and *Setaria*-db, a comprehensive database for *Setaria*. *Mol. Plant* **17**, 219–222.
- Tian, J., Wang, C., Chen, F., Qin, W., Yang, H., Zhao, S., Xia, J. *et al.* (2024) Maize smart-canopy architecture enhances yield at high densities. *Nature* **632** (8025), 576–584.
- Walsh, J., Waters, C. and Freeling, M. (1998) The maize gene *liguleless2* encodes a basic leucine zipper protein involved in the establishment of the leaf blade-sheath boundary. *Genes Dev.* **12**, 208–218.
- Wang, R., Liu, C., Chen, Z., Sun, S. and Wang, X. (2021) *Oryza sativa* *LIGULELESS 2s* determine lamina joint positioning and differentiation by inhibiting auxin signaling. *New Phytol.* **229**, 1832–1839.
- Yu, Y. (2019) *Liguleless1*, a conserved gene regulating leaf angle and a target for yield improvement in wheat. *Plant Physiol.* **181**, 4–5.
- Zhang, R., Jia, G. and Diao, X. (2023) geneHapR: an R package for gene haplotypic statistics and visualization. *BMC bioinformatics* **24**, 199.
- Zhao, M., Tang, S., Zhang, H., He, M., Liu, J., Zhi, H. *et al.* (2020) *DROOPY LEAF1* controls leaf architecture by orchestrating early brassinosteroid signaling. *Proc. Natl. Acad. Sci. U. S. A.* **117**, 21766–21774.

Supporting information

Additional supporting information may be found online in the Supporting Information section at the end of the article.

Appendix S1 Supplemental Materials and Methods.

Figure S1–S8 Supplementary Figures.

Table S1–S5 Supplementary Tables.